HHS Public Access

Author manuscript

J Mater Chem B. Author manuscript; available in PMC 2023 November 09.

Published in final edited form as:

J Mater Chem B. ; 10(43): 8970–8980. doi:10.1039/d2tb01343f.

Size effect of liposomes on centimeter-deep ultrasound-switchable fluorescence imaging and ultrasound-controlled release

Yang Liu[1,2,#], **Tingfeng Yao**[1,2,#], **Liqin Ren**[1,2], **Baohong Yuan**[1,2,*]

[1]Department of Bioengineering, The University of Texas at Arlington, TX 76010, USA. Joint Biomedical Engineering Program, The University of Texas at Arlington and University of Texas Southwestern Medical Center, Dallas, TX 75235, USA

[2]Ultrasound and Optical Imaging Laboratory, Department of Bioengineering, The University of Texas at Arlington, Arlington, TX 76010, USA

Abstract

Liposomes have been widely used in both medical imaging and drug delivery fields due to their excellent biocompatibility and easy surface modification. Recently our lab reported the first-time implementation of temperature-sensitive and indocyanine green (ICG)-encapsulated liposome microparticles for *in vivo* ultrasound-switchable fluorescence (USF) imaging. A previous study showed that liposomes microparticles achieved USF imaging in centimeters-deep tissue. This study aimed to control the size of liposomes in the nanoscale and study the size effect on USF imaging depth. Also, we explored the feasibility of combining USF imaging with an ultrasound-controlled release. Liposomes were synthesized via the hydration method and the size was controlled with an extruding process. Characterizations, including fluorescence profile, spectra, size, stability, encapsulation efficiency, and ultrasound-controlled release, were evaluated. USF imaging in blood serum was conducted successfully in a phantom model, and an imaging depth study was conducted at 1.0 cm and 2.5 cm and confirmed that nano-sized liposomes had a stronger USF signal than micron-sized liposomes. Additionally, releasing tests indicated that both ultrasound power and exposure time affected release efficiency that increasing the power and extending the exposure time led to higher release efficiency. Above all, this study shows the potential for using liposomes for USF imaging and ultrasound-controlled release.

Graphical Abstract

[*]Corresponding author's baohong@uta.edu. (B. Yuan).
[#]These authors contributed equally to this work.

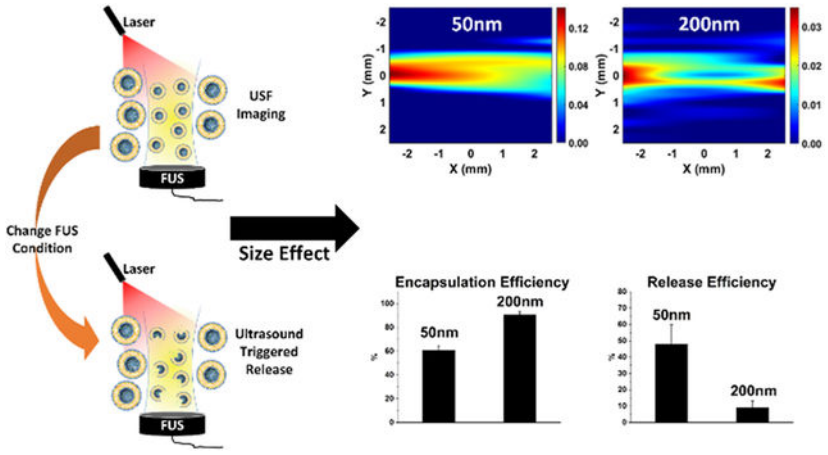

Study achieved centimeter-deep ultrasound switchable fluorescence (USF) imaging and ultrasound assisted release *in vitro* with indocyanine green dye encapsulated liposome nanoparticles (ICG-liposomes). Size effect of ICG-liposomes on both USF imaging and ultrasound assisted release has been studied and it provided support for future *in vivo* application.

Keywords

liposomes; size; ultrasound-switchable fluorescence; ultrasound-controlled release

1. Introduction

Fluorescence imaging is a major biomedical imaging technology that has been used for drug delivery tracking, disease diagnoses, *in vivo* molecular dynamics study, and treatment evaluation.[1-3] However, conventional fluorescence imaging using near-infrared (NIR) fluorophores with a wavelength in the first window (NIR-I, 700-900 nm) suffers from low spatial resolution (such as a few millimeters) in centimeters-deep tissue due to tissue significant light scattering. One of the methods to improve the imaging resolution (such as sub-millimeters or better) is to reduce the light scattering by adopting a longer wavelength, such as using a fluorophore with an emission wavelength in the second NIR window (NIR-II, 1,000-1,700 nm). According to a recent report, this goal was achieved at an imaging depth of 1.5 cm in live biological tissue via a novel NIR-II fluorophore (excited at 808 nm and detected at >1250 nm).[4] However, the benefit of using NIR-II fluorophores compared to NIR-I fluorophores faded (or limited), worsening when targeting much deeper tissue (such as >2 cm). This is mainly because the absorption of water and lipid is much stronger at NIR-II and limits its penetration depth in live tissue.[5] We developed the ultrasound-switchable fluorescence (USF) imaging technique in our lab and attained a high spatial resolution in centimeters-deep tissue using USF contrast agents containing NIR-I fluorophores (but not limited to NIR-I fluorophores).[6,7] The USF working principle involves using a focused ultrasound (FUS) transducer to heat a small region, and only the temperature-sensitive contrast agents within this region are switched on due to size reduction and change of microenvironment inside contrast agents, leading to an increase in the fluorescence emitted by the agents. The spatial resolution of the USF imaging is determined by the focal size of

the FUS transducer and contrast agents play an important role in determining USF signal strength and imaging depth. Reducing both scattering and tissue absorption will improve USF signal strength and imaging depth. Usually, light absorption is the major limiting factor of the USF signal strength and imaging depth in much deeper tissue (such as >2 cm). Compared to computed tomography, which usually need the help from radioactive contrast agent for targeting imaging, the contrast agent used for USF imaging is safer and does not involve radioactive beam. Compared to conventional ultrasound, USF technique can not only image in centimeter-deep tissue with high resolution, but also apply potential multicolor imaging techniques to identify different targeting objects.

Currently, three major types of contrast agents are used for USF imaging, including micelles, polymer-based nanogel, and liposomes. The micelle, a single lipid layer particle, showed an incredibly high fluorescence intensity on-to-off ratio of more than 200.[8] In addition, successful USF imaging was conducted under a 3.1 cm thick porcine tissue. However, the micelle's structure was unstable after mixing with mouse blood, which prevented it from *in vivo* USF imaging. The second well-developed contrast agent was a thermosensitive polymer-based nanogel, poly(N-isopropylacrylamide) (PNIPAM).[9] It has outstanding stability and can be stored for a year or longer.[10] More importantly, its USF property remains in biological environments (such as in blood or tissue fluids) and has been successfully demonstrated for *in vivo* USF imaging of mouse muscles and organs (such as livers and spleens) via either a local or an intravascular injection.[11,12] Recently, the PNIPAM-based contrast agent was further refined by shifting the emission peak from 610 nm to 790 nm, resulting in a stronger USF signal.[13] Modification of PNIPAM-based nanoparticles were investigated and pH sensitive PNIPAM nanoparticles were obtained that USF fluorescence intensity increases while in low pH environment.[14] Nevertheless, the biocompatibility of PNIPAM-based agents is a potential concern.[15,16] To improve biocompatibility, indocyanine green (ICG)-encapsulated liposomes, which comprise biocompatible lipids, were developed. A higher fluorescence intensity change was observed compared to that of the PNIPAM nanogels, and a successful *in vivo* USF imaging was conducted in the liver.[6,17] However, the liposomes were around 6.5 μm in size, which was too large and limited the *in vivo* usage.

Liposomes have been widely used as a drug carrier because of their outstanding advantages, including biocompatibility, self-assemble capability, feasibility to load both polar and nonpolar drugs, and easy surface modification for molecular targeting. For example, doxorubicin (DOX)-encapsulated liposomes were used for targeted drug delivery.[18-20] However, the lack of drug release control is considered an issue.[21] Ultrasound-mediated drug release of liposomes is one of the potential solutions to overcoming this barrier.[22,23] Studies on liposome structure modification via PEGylation on the surface found increased efficiency of liposomes broken via ultrasound.[24] Combining imaging with liposome drug release provides a controllable drug delivery option, and a recent report showed the success of using fluorescence imaging to confirm the accumulation of liposomes in a tumor before conducting a temperature-triggered drug release.[25]

Liposome's size plays a vital role in *in vivo* applications such as imaging and drug delivery. It is well-known that liposomes can be used as a carrier to protect active ingredients from

rapid clearing from the body and its size affects *in vivo* biodistribution and circulation time in mice.[26] Liposomes sized between 150 nm and 200 nm have decreased liver uptake and prolonged circulation time in mice. In contrast, liposomes with a size greater than 300 nm have shorter circulation time and tend to accumulate in the spleen. In addition, liposomes with a size less than 70 nm have comparable circulation time to liposomes with a size greater than 300 nm, but they do not accumulate in the spleen and have higher uptake in the liver.[27,28] Also, the size of liposomes is known to affect the encapsulation efficiency.[29] The encapsulation efficiency of liposomes with sizes smaller than 50 nm may be limited due to the smaller volume.[30] Furthermore, the toxicity of liposomes increases as the size increases.[31]

A combination of USF imaging with ultrasound-controlled release using liposomes as both imaging contrast agents and content carriers is proposed in this study. Various sizes of liposomes were synthesized, and the surface of the liposomes was decorated with PEGylated chains with a folate functional group at the end of the chain to enhance physiological stability and to increase ultrasound breaking efficiency and potential future folate targeting. The relationship between the emitted fluorescence intensity and temperature was examined with an in-house built cuvette system. Both excitation and emission spectra were measured with a spectrometer, and the hydrodynamic size was studied using a dynamic light scattering (DLS) particle analyzer. The size effect of liposomes on USF imaging depth was studied with a chicken breast tissue stacked phantom model. Finally, the release efficiency was examined under FUS powers and exposure times. Results showed that liposomes can be potentially used for centimeters-deep tissue USF imaging and drug delivery application.

2. Experimental

2.1 Liposome synthesis

The schematic diagram of synthesizing ICG-encapsulated liposomes (ICG-liposomes) is shown in Figure 1. Both 5 mg of 1,2-dipalmitoyl-sn-glycero-3-phosphocholine (DPPC) and 0.22 mg of 1,2-distearoyl-sn-glycero-3-phosphoethanolamine-N-[folate(polyethylene glycol)-2000] (DSPE-PEG2000-Folate) were dissolved in 2 mL chloroform (98 %, Fisher Scientific International, Inc., USA). A rotor evaporator (R300, BUCHI, Corp., USA) was used to completely evaporate chloroform at 55 °C, −85 kPa, and 120 rpm in 30 min. A thin layer of lipid film formed on the wall of the flask. Then, 0.8 mL of pre-warmed ICG (≥96 % HPLC, Fisher Scientific International, Inc., USA) aqueous solution (0.07 mg/mL) was pipetted into the flask and swirled in a water bath at 55 °C for 30 seconds, followed with hydrolyzing lipids in a rotor evaporator at 42 °C and 120 rpm for 1 hr. The micron-sized ICG-liposomes were collected and stored at 4 °C. Next, the size of the ICG-liposomes was reduced and controlled via the extrusion method. The desired polycarbonate filter disk size (30 nm, 50 nm, 100 nm, or 200 nm) was selected and installed in the mini-extruder (Avanti Polar Lipids Inc., USA) with two filter supports. The filter disk was pre-wetted with deionized (DI) water before extruding. The ICG-liposomes were aspirated to a gas-tight 1 mL syringe and inserted to the mini-extruder. Another empty syringe was inserted to the other end of the mini-extruder. The assembled mini-extruder apparatus was placed in a pre-heated (50 °C) heating block and waited for 10 min for temperature of the solution to

equilibrate. Afterward, the ICG-liposomes were filtered 19 times. When filtering with both the 30 nm and 50 nm filter disks, a pre-filtering using the 100 nm filter disk was required. Next, the obtained ICG-liposomes were dialyzed against DI water at 4 °C for 24 h to remove free lipids and free ICG dye molecules. The final volume of ICG-liposomes was adjusted to 3.5 mL using DI water. Finally, the ICG-liposomes were stored in a sealed container at 4 °C and used within 2 days. Both DPPC and DSPE-PEG200-Folate were purchased from Avanti Polar Lipids, Inc., USA.

2.2 Liposome characterization

The effectiveness of ICG-liposomes as a USF imaging contrast agent was evaluated via an in-house built cuvette system.[6] Briefly, 3 mL of ICG-liposomes were transferred into a 3.5 mL quartz cuvette (Hellma, Germany), which was placed inside a temperature-controlled holder (Quantum Northwest, Inc., USA). An 808 nm laser (MGL-II-808-2W, Dragon Lasers, China) was used as excitation light to excite ICG-liposomes. The emission light was passed through an 830 nm long-pass (LP) filter (Semrock, USA) before being collected by a modular USB spectrometer (USB2000+, Ocean Inlight, USA). The emitted fluorescence intensity changed with respect to the change in temperature and was recorded with a temperature increment of 0.1 °C. In addition, the stability of ICG-liposomes was evaluated with the effects of ionic strength and pH using the cuvette system. A potassium chloride (KCl) solution with different concentrations (0, 25, 50, 100, 150, and 200 mM) or an aqueous solution with various pH (5.2, 6.3, 7.4, and 9.2) were mixed with ICG-liposomes in a 5:1 ratio (v/v), accordingly. More, to further study the stability of ICG-liposomes in physiological condition, the mouse blood serum (BioIVT, USA) was mixed with ICG-liposomes (1:1 v/v), and the fluorescence intensity change with respect to the change in temperature was measured using the cuvette system.

The hydrodynamic size of ICG-liposomes was measured using the DLS particle analyzer (NanoBrook 90PlusPALS, Brookhaven Instruments, USA). The incident angle of the 659 nm laser was 90°. Samples were diluted with DI water until the count rate reached 300–700 kcps, and the temperature was set at 25 °C. Measurement was repeated three times. The excitation and emission spectra of ICG-liposomes were characterized via a spectrometer (Fluoromax-Plus-C, Horiba, Japan) using a 300 μL quartz cuvette (Hellma, Germany) and stirring at 25 °C. The excitation spectrum was scanned from 650–810 nm with an 830 nm LP emission filter and an emission recording wavelength at 850 nm. The emission spectrum was acquired using a 530 nm excitation light and a 550 nm LP emission filter (Semrock, USA) and recorded from 650–850 nm.

2.3 USF imaging: tube model and depth study

The setup of the frequency-domain USF imaging system has been demonstrated in previous published works and the schematic diagram is shown in Figure S1.[32] The effectiveness of the ICG-liposomes for USF imaging was evaluated using a tube phantom model. Briefly, a silicone tube (ST 60-011-01, Helix Medical, USA) with an inner diameter of 0.31 mm and an outer diameter of 0.64 mm was inserted through the bottom of a silicone phantom, which had a thickness of 0.8 cm. The silicone phantom was prepared with addition of 0.06 mg/mL titanium dioxide as a scattering medium. Then, the tube model was immersed

into a 37 °C water tank to mimic the body temperature. The USF imaging was conducted with various sized ICG-liposomes mixed with either DI water or mouse blood serum (1:1 v/v). The mixture was injected into the tube and waited for 10 min to equilibrate the temperature. A 2.5 MHz FUs transducer (H-108, Sonic Concepts Inc., USA) was mounted at the bottom of the water tank and focused on the silicone tube. The FUS was used to elevate temperature and switch on the ICG-liposomes within the focal volume. The estimated FUS power used during USF imaging was 0.19 W, and the mechanical index (MI) was 0.97. The scan area was 5.08 mm × 5.08 mm, and the step sizes were 2.54 mm and 0.254 mm in X and Y directions, respectively. A 785 nm laser (MDL-III-785-2W, CNI, China) was used as the excitation light (121 μW/cm^2) and filtered through a 785/62 nm band-pass filter (Semrock, USA). The excitation light intensity was measured using a power and energy meter (PM100D, Thorlabs, Germany). The emission light was collected using a fiber bundle and passed through one 830 nm absorption filter (Semrock, USA) and two 830 nm LP filters before being collected by a photomultiplier tube (H7422-20, Hamamatsu, Japan).

A depth study was conducted using the tube model with different thicknesses (1.0 cm and 2.5 cm) of chicken breast tissue stacked on top of the phantom. Similarly, various sized ICG-liposomes were injected into the tube and conducted USF imaging with the same scan area and step sizes. The FUS power was 0.77 W (MI: 1.93), and the laser intensity was 544 μW/cm^2 and 7.6 mW/cm^2 for USF imaging at 1.0 cm and 2.5 cm thicknesses, respectively.

2.4 Releasing test and encapsulation efficiency

The ultrasound triggered releasing test was studied by adding 500 μL ICG-liposomes into a cylindrical vessel with bottom sealed with parafilm and top enclosed with a rubber stopper. Then, the vessel was immersed into a 37 °C water bath. A 2.5 MHz FUS transducer was fixed at the bottom of the water tank and focused on the solution. A pulsed cycle (pulse repetition period: 15s, pulse on: 400 ms) was generated using a function generator (33500B, Agilent, USA) and amplified by a 50 dB-gain radio frequency power amplifier (A075, E&I, USA). Three different ultrasound powers of 0.19 W (MI: 0.97, P1), 1.74 W (MI: 2.90, P2), and 4.82 W (MI: 4.83, P3) were implemented to break liposomes. A two-dimensional scan was conducted using a three-axis motorized translational stage (XSlide™ and VXM™, Velmex Inc., USA) to mimic a USF imaging scenario. The scanning area was 5.08 mm x 5.08 mm with a step size of 0.508 mm in both X and Y directions. After scanning, the ICG-liposomes were transferred into a 1.5 mL microcentrifuge tube and centrifuged at 10,000 xg for 45 min at 4 °C. The intact ICG-liposomes were sedimented at bottom of the tube, and the released ICG was dispersed in the solution, which was then transferred into a 300 μL quartz cuvette, and the fluorescence intensity was measured using the spectrometer. In addition, to study the effects of ultrasound exposure time on breaking liposomes, scanning was repeated five times with ultrasound power of 4.82 W (P4). To exclude the effect of temperature on ICG-liposomes' destruction and preexisting free ICG influence, a negative control, which was not exposed with ultrasound, was kept at 37 °C for a corresponding scanning time. More, a positive control (100 % release) with completely broken ICG-liposomes solution was prepared using a sonic dismembrator (FB505, Fisher Scientific, USA) with 20 % power and 30 % duty cycle for 3 minutes in an ice bath. For all releasing tests, the ultrasound triggered content release percent was quantified using Equation 1.

$$\text{Ultrasound Triggered Release } \% = \frac{S - NC}{PC - NC} \times 100\,\% \quad \text{(Equation 1)}$$

S: fluorescence intensity of sample, counts

NC: fluorescence intensity of negative control, counts

PC: fluorescence intensity of positive control, counts

The ICG encapsulation efficiency was calculated via Equation 2. After synthesizing ICG-liposomes, the unencapsulated ICG was separated from ICG-liposomes via centrifugation. Then, a spectrometer was used to acquire the fluorescence intensity of the unencapsulated ICG. Meanwhile, an ICG aqueous solution, which had the same concentration used during ICG-liposomes synthesis (0.016 mg/mL), was prepared, and the fluorescence intensity was measured.

$$\text{Encapsulation Efficiency } \% = \left(1 - \frac{\text{Unencapsulated ICG}}{\text{ICG solution}}\right) \times 100\,\% \quad \text{(Equation 2)}$$

3. Results

The ICG-encapsulated and thermosensitive liposomes were synthesized via the hydration method, and the size of liposomes controlled via extrusion approach. To evaluate the USF imaging feasibility of the ICG-liposomes, the fluorescence intensity profile, which showed the relationship between the change of fluorescence intensity and the change of temperature, was studied. Factors such as background fluorescence intensity, lower critical solution temperature (LCST) or switch on temperature, fluorescence intensity on-to-off ratio, absolute fluorescence intensity change, and transition temperature range are critical to assessing the USF imaging capability for a contrast agent. The fluorescence intensity profile is shown in Figure 2a and 2b for both filtered and unfiltered ICG-liposomes. It is clear to state that the fluorescence intensity gradually increases first, followed by a sharp upsurge within the narrow transition temperature range, and finally levels off. According to the normalized data shown in Figure 2b, the shape of the fluorescence intensity profiles was similar for different sized ICG-liposomes. A linear relationship between the hydrodynamic size measured with the DLS and the filter size used during extrusion is indicated in Figure 2c. The ICG-liposomes had hydrodynamic sizes of 82.3, 94.0, 117.7, and 162.4 nm after extrusion with 30, 50, 100, and 200 nm filter disks, respectively. The TEM image shows a round shape of the ICG-liposomes (Figure S2). According to Figure 2d, smaller ICG-liposomes tended to have stronger background fluorescence. Figure 2e shows that the filtered or nano-sized ICG-liposomes had lower LCSTs around 38.8 °C, and the unfiltered or micron-sized ICG-liposomes had an LCST at 40.4 °C. The on-to-off ratio with respect to the size of ICG-liposomes is presented in Figure 2f, and no obvious difference was observed between various sized ICG-liposomes. Further stability result showed that 200 nm filtered ICG-liposomes remained stable within 3 on/off cycles. The absolute fluorescence intensity difference between switch on and off is one of the key factors that determines

the potential USF imaging depth of contrast agents. An obvious decrease in absolute fluorescence intensity difference is recognized as the size of ICG-liposomes increase (Figure 2g). Figure 2h shows that nano-sized ICG-liposomes had a higher transition temperature range compared to that of micron-sized ICG-liposomes.

Because the high temperature (50 °C) applied on ICG-liposomes during the extrusion process might accelerate the degradation of ICG dye and cause a shift of emission spectrum, it is necessary to characterize the spectrum of ICG-liposomes.[33] Figures 3b and c show the excitation and emission spectra of ICG-liposomes, respectively. Apparently, the size of ICG-liposomes does not affect the spectra. As shown in Figure S3, the temperature has no effect on the emission spectrum of ICG-liposomes. In addition, compared to the spectra of fresh ICG aqueous solution (Figure 3a), we confirmed that the degradation of ICG dye was negligible, and a slight red shifting can be noted for the emission peak of ICG-liposomes from 809 nm to 831 nm.

Figure 4 summarizes the effect of ionic strength and pH on the fluorescence profile of different-sized ICG-liposomes. As shown in Figure 4a, b, c, and d, the shape of the fluorescence intensity profile remains unchanged as the concentration of KCl solution increased from 0 mM to 200 mM. It indicates that ICG-liposomes were stable in solution with different ionic strengths. In addition, it is well-known that the pH level varies in different human body fluids and tissues.[34] Thus, it is essential to study the stability of ICG-liposomes in solution with different pH values. Figure 4e, f, g, and h demonstrate that ICG-liposomes were stable within a pH range from 5.2 to 9.2.

The *ex vivo* USF imaging with a tube model is shown in Figure 5. Both the fluorescence profile and USF imaging of ICG-liposomes mixed with either blood serum or DI water were investigated. The fluorescence profile shows that after mixing with blood serum, the LCST slightly shifted to the left at around 37 °C, and the absolute fluorescence intensity difference between switch on/off increased. Furthermore, we can clearly identify the location and shape of the silicone tube with USF imaging of ICG-liposomes mixed with either water or blood serum. After mixing the LNPs with blood serum, the fluorescence intensity of USF imaging increased as the size of ICG-liposomes decreased.

According to the cuvette results reported in Figure 2 and the USF imaging results presented in Figure 5, the size of ICG-liposomes affected the USF imaging signal strength relating to the depth limit of USF imaging. Thus, a USF imaging depth study was conducted to compare USF imaging signal strength at both 1.0 cm and 2.5 cm for different-sized ICG-liposomes. Figure 6a and b exhibit images of silicone tube embedded phantoms with 1.0 cm and 2.5 cm thick chicken breast tissues stacked on top, respectively. Figure 6c shows that 30 nm filtered ICG-liposomes had the highest USF signal strength at a depth of 1.0 cm, and unfiltered or micron-sized ICG-liposomes had the lowest USF signal strength. After increasing the tissue thickness from 1.0 cm to 2.5 cm, we barely detected the USF signal from the unfiltered ICG-liposomes but still recognized USF signals from nano-sized ICG-liposomes. Again, 30 nm filtered ICG-liposomes had the strongest USF signal strength at 2.5 cm.

As presented in Figure 7a, large-sized ICG-liposomes (100 nm and 200 nm filtered) had a higher encapsulation efficiency of more than 80 %, and small-sized ICG-liposomes (30 nm and 50 nm filtered) possessed an encapsulation efficiency of 60 %. For ultrasound-triggered releasing tests, four FUS power conditions were examined. Condition P1 mimicked the FUS power used during USF imaging. According to Figure 7b, 7.38 ± 1.85 % release was observed for 50 nm filtered ICG-liposomes in condition P1, and the ICG release for 200 nm filtered ICG-liposomes was only 0.89 ± 1.13 %. After increasing FUS powers, we can clearly see the ICG release increased to 13.47 ± 2.36 % (condition P2) and 24.56 ± 5.92 % (condition P3) for 50 nm filtered ICG-liposomes. Also, the ICG-release increased to 4.53 ± 2.69 % (condition P2) and 5.09 ± 1.07 % (condition P3) for 200 nm filtered ICG-liposomes. The results state that by increasing the FUS power, we can achieve higher ICG release. Furthermore, instead of increasing the power of FUS, extending the exposure time to five times more and keeping the FUS power the same as condition P3 can also increase the ICG release dramatically (condition P4). The ICG release reached 48.01 ± 11.76 % and 9.17 ± 3.85 % for 30 nm and 200 nm filtered ICG-liposomes, respectively. In general, 50 nm filtered ICG-liposomes had a higher ultrasound-triggered release in comparison with that of the 200 nm filtered ICG-liposomes.

4. Discussion

The contrast agents for USF imaging have constraints for both dyes and vesicles. First, the dye should be polarity sensitive while having a high quantum yield in a low polarity environment and low quantum yield in a high polarity condition.[9] Next, the vesicle used to encapsulate the dye needs to be thermal sensitive so that the vesicle shrinks when the temperature increases to create a relatively low polarity environment to increase the fluorescence intensity of the dye [17,35,36]. In addition, because the vesicle is flexible enough to change size with respect to a change of temperature, the vesicle should also be stable so that increasing temperature and exposing them to ultrasound mechanical force and the physiological environment will not break it. Note that unilamellar and nano-sized liposomes have abundant features including feasibility to cross biological barriers such as the blood-brain barrier[37] and excellent enhanced permeability and retention effect for passive accumulation in tumor cells compared to that of multilamellar and micron-sized liposomes.[38] In addition, liposomes, within 20–200 nm, exhibit better cellular targeting efficiency, and nano-sized liposomes are also favored for vaccine application because only liposomes in the nanometer range can reach lymph nodes and directly contact with B cells.[39] These properties of nano-sized liposomes provide potential applications such as targeted USF imaging. Therefore, nano-sized liposomes were synthesized and the eligibility for USF imaging was assessed. Despite unilamellar and nano-sized liposomes having extensive advantages compared with multilamellar and micron-sized liposomes, the unilamellar and nano-sized liposomes are considered more vulnerable due to their single bi-layer structure. The polyethylene glycol chain can be decorated on the surface of liposomes to improve stability by preventing self-aggregation and prolonging circulation time.[40,41]

The nano-sized ICG-liposomes had a higher absolute fluorescence intensity change between switch on/off compared to that of micron-sized ICG-liposomes. This indicates that nano-sized ICG-liposomes tend to have a stronger USF signal strength and are therefore suitable

for deeper USF imaging, which was confirmed by the depth study. Although micron-sized ICG-liposomes were eligible for USF imaging at 1 cm deep with reasonable signal strength, nano-sized ICG-liposomes had greater USF signal strength and can be used for USF imaging at 2.5 cm deep. Additionally, nano-sized liposomes had LCSTs around 38.8 °C, which was closer to the body temperature than the LCST (40.4 °C) of micron-sized liposomes. This is beneficial for potential *in vivo* USF imaging because less ultrasound energy was needed to switch on the contrast agent, and therefore it is safer to implement. The fluorescence emission intensity from nano-sized liposomes was found to be stronger than that of micron-sized liposomes. This feature could be useful when fluorescence imaging is needed at first to roughly localize the region of interest. It is worth it to note that after decreasing the size of ICG-liposomes, the temperature transition bandwidth increased from 1.4 °C to around 2.5 °C. This means higher thermal energy is needed to fully switch on the ICG-liposomes. Furthermore, the emission peak of ICG-liposomes shifted from 809 nm to 831 nm, which is desired because the tissue absorption and autofluorescence interference are minimized.

The ability to monitor the accumulation and releasing status of liposomes in the centimeter-deep tissue is valuable. The combination of USF imaging with ultrasound-controlled release offered an opportunity to achieve this goal. ICG-liposomes were proved to be stable enough and eligible for USF imaging in the tube model after mixing with blood serum using a FUS power of 0.19 W (MI 0.97). This FUS power caused only 7.38 % and 0.89 % release of ICG for 200 and 50 nm ICG-liposomes, respectively. By either increasing the FUS power or exposure time, the higher release quantity can be attained. Thus, implementing USF imaging to monitor the accumulation of ICG-liposomes and initiating release by increasing FUS intensity and exposure time is feasible. In addition, the size effect on the release percentage and loading efficiency was observed. A trade-off was expected because large-sized ICG-liposomes (200 nm filtered) had a higher encapsulation efficiency, but a lower release percentage. Thus, large-sized ICG-liposomes were more suitable for application of slow release with high encapsulating quantity, and small-sized ICG-liposomes were applicable for quick and sudden release in low quantity.

The results of this study confirmed that nano-sized ICG-liposomes has a strong USF signal, can image in 2.5 cm deep tissue, has an LCST close to body temperature, and has a red-shifted emission spectrum. The integration of USF imaging and ultrasound-controlled release opens possibilities for applications such as monitoring the accumulation of liposomes in centimeters-deep tissue and releasing encapsulated drugs with the help of ultrasound when desired. One of the limitations is that the shelf life was reduced compared to micron-sized ICG-liposomes. Sugars, such as sucrose and isomaltose, could be added in the nano-sized ICG-liposome solution for a possible longer shelf life.[42] This study also led to great potentials for future research, such as *in vivo* folate-targeted USF imaging and ultrasound-controlled drug release for tumor imaging and treatment.

5. Conclusion

The thermosensitive and PEGylated liposomes encapsulated with ICG were first implemented for USF imaging, and various sizes of ICG-liposomes were characterized.

Compared to micron-sized ICG-liposomes, nano-sized ICG-liposomes had an LCST shifted to 38 °C, which is beneficial for *in vivo* applications. The fluorescence intensity profile indicates that small ICG-liposomes have a stronger fluorescence emission and therefore a higher absolute value of fluorescence intensity change. These features allow ICG-liposomes to reach centimeters-deep tissue USF imaging. ICG-liposomes also showed an outstanding stability in solution with various ionic strengths and pH values, and USF imaging was successfully conducted after mixing with blood serum. In addition, a depth study showed that nano-sized ICG-liposomes can conduct USF imaging in deeper tissue compared to that of micron-sized ICG-liposomes. Moreover, the feasibility of combining USF imaging with ultrasound-controlled release was verified in this study. Although negligible release was noticed during USF imaging with a FUS power of 0.19 W (MI: 0.97), increasing FUS power and exposure time could lead to an obvious increase of the release. Above all, this study led to the future potential of high-resolution USF imaging guided and ultrasound-controlled drug release in centimeters-deep tissue using the ICG-liposomes.

Supplementary Material

Refer to Web version on PubMed Central for supplementary material.

Acknowledgement

This work was supported in part by funding from the NIH/NIBIB 1R15EB030809-01 (Baohong Yuan), CPRIT RP170564 (Baohong Yuan) and the REP 270089 (Baohong Yuan). Thanks to Dr. Kytai T. Nguyen for her generous offer for us to use the DLS instrument.

References

(1). Hassan M; Klaunberg BA Biomedical Applications of Fluorescence Imaging in Vivo. Comp. Med 2004, 54 (6), 635–644. [PubMed: 15679261]

(2). Yukawa H; Baba Y In Vivo Fluorescence Imaging and the Diagnosis of Stem Cells Using Quantum Dots for Regenerative Medicine. Anal. Chem 2017, 89 (5), 2671–2681. 10.1021/acs.analchem.6b04763. [PubMed: 28194939]

(3). Engelhard S; van Helvert M; Voorneveld J; Bosch J; Jebbink EG; Versluis M; Reijnen M First-in-Human Results of Ultrasound Velocimetry for Visualization of Blood Flow Patterns in Patients with Peripheral Arterial Disease. Eur. J. Vasc. Endovasc. Surg 2019, 58 (6), e805–e806. 10.1016/j.ejvs.2019.09.398.

(4). Sheng Z; Li Y; Hu D; Min T; Gao D; Ni J-S; Zhang P; Wang Y; Liu X; Li K; Zheng H; Tang BZ Centimeter-Deep NIR-II Fluorescence Imaging with Nontoxic AIE Probes in Nonhuman Primates. Research 2020, 2020, 1–14. 10.34133/2020/4074593.

(5). Sun A; Guo H; Gan Q; Yang L; Liu Q; Xi L Evaluation of Visible NIR-I and NIR-II Light Penetration for Photoacoustic Imaging in Rat Organs. Opt. Express 2020, 28 (6), 9002. 10.1364/oe.389714. [PubMed: 32225514]

(6). Yao T; Liu Y; Ren L; Yuan B Improving Sensitivity and Imaging Depth of Ultrasound-Switchable Fluorescence via an EMCCD-Gain-Controlled System and a Liposome-Based Contrast Agent. Quant. Imaing Med. Surg 2020, 20 (796), 1–12. 10.21037/qims-20-796.

(7). Yuan B; Uchiyama S; Liu Y; Nguyen KT; Alexandrakis G High-Resolution Imaging in a Deep Turbid Medium Based on an Ultrasound-Switchable Fluorescence Technique. Appl. Phys. Lett 2012, 101 (3), 033703. 10.1063/1.4737211.

(8). Cheng B; Bandi V; Wei MY; Pei Y; D'Souza F; Nguyen KT; Hong Y; Yuan B High-Resolution Ultrasound-Switchable Fluorescence Imaging in Centimeter-Deep Tissue Phantoms with High

Signal-to-Noise Ratio and High Sensitivity via Novel Contrast Agents. PLoS One 2016, 11 (11), 1–16. 10.1371/journal.pone.0165963.

(9). Cheng B; Wei MY; Liu Y; Pitta H; Xie Z; Hong Y; Nguyen KT; Yuan B Development of Ultrasound-Switchable Fluorescence Imaging Contrast Agents Based on Thermosensitive Polymers and Nanoparticles. IEEE J Sel Top Quantum Electron 2015, 20 (6), 1588–1595. 10.4172/2157-7633.1000305.Improved.

(10). Yu S; Cheng B; Yao T; Xu C; Nguyen KT; Hong Y; Yuan B New Generation ICG-Based Contrast Agents for Ultrasound-Switchable Fluorescence Imaging. Sci. Rep 2016, 6, 35942. 10.1038/srep35942. [PubMed: 27775014]

(11). Yao T; Yu S; Liu Y; Yuan B In Vivo Ultrasound-Switchable Fluorescence Imaging. Sci. Rep 2019, 9 (1), 1–13. [PubMed: 30626917]

(12). Yu S; Yao T; Liu Y; Yuan B In Vivo Ultrasound-Switchable Fluorescence Imaging Using a Camera-Based System. Biomed. Opt. Express 2020, 11 (3), 1517–1538. [PubMed: 32206426]

(13). Liu R; Yao T; Liu Y; Yu S; Ren L; Hong Y; Nguyen KT; Yuan B Temperature-Sensitive Polymeric Nanogels Encapsulating with β-Cyclodextrin and ICG Complex for High-Resolution Deep-Tissue Ultrasound-Switchable Fluorescence Imaging. Nano Res. 2020, 13 (4), 1100–1110.

(14). Saremi B; Yao T; Yuan B Thermo- and PH-Sensitive Nanoparticles of Poly (N-Isopropylacrylamide-Decenoic Acid-1-Vinylimidazole) for Ultrasound Switchable Fluorescence Imaging. Exp. Biol. Med 2022, 1005–1012. 10.1177/15353702221087648.

(15). Wadajkar AS; Koppolu B; Rahimi M; Nguyen KT Cytotoxic Evaluation of N-Isopropylacrylamide Monomers and Temperature-Sensitive Poly(N-Isopropylacrylamide) Nanoparticles. J. Nanoparticle Res 2009, 11 (6), 1375–1382. 10.1007/s11051-008-9526-5.

(16). Deka SR; Quarta A; Di Corato R; Riedinger A; Cingolani R; Pellegrino T Magnetic Nanobeads Decorated by Thermo-Responsive PNIPAM Shell as Medical Platforms for the Efficient Delivery of Doxorubicin to Tumour Cells. Nanoscale 2011, 3 (2), 619–629. 10.1039/c0nr00570c. [PubMed: 21082085]

(17). Liu Y; Yao T; Cai W; Yu S; Hong Y; Nguyen KT; Yuan B A Biocompatible and Near-Infrared Liposome for In Vivo Ultrasound-Switchable Fluorescence Imaging. Adv. Healthc. Mater 2020, 9 (4), 1–10. 10.1002/adhm.201901457.

(18). Du Y; Liang X; Li Y; Sun T; Jin Z; Xue H; Tian J Nuclear and Fluorescent Labeled PD-1-Liposome-DOX-64Cu/IRDye800CW Allows Improved Breast Tumor Targeted Imaging and Therapy. Mol. Pharm 2017, 14 (11), 3978–3986. 10.1021/acs.molpharmaceut.7b00649. [PubMed: 29016143]

(19). Belhadj Z; Ying M; Cao X; Hu X; Zhan C; Wei X; Gao J; Wang X; Yan Z; Lu W Design of Y-Shaped Targeting Material for Liposome-Based Multifunctional Glioblastoma-Targeted Drug Delivery. J. Control. Release 2017, 255, 132–141. 10.1016/j.jconrel.2017.04.006. [PubMed: 28390902]

(20). Hossann M; Hirschberger J; Schmidt R; Baumgartner C; Zimmermann K; Baer S; Ratzlaff C; Peller M; Troedson K; Limmer S; Brühschwein A; Dörfelt R; Kreutzmann N; Wess G; Knösel T; Schagon O; Fischer J; Grüll H; Willerding L; Schmidt M; Meyer-Lindenberg A; Issels RD; Schwaiger M; Eggermont AM; ten Hagen TL; Lindner LH A Heat-Activated Drug-Delivery Platform Based on Phosphatidyl-(Oligo)-glycerol Nanocarrier for Effective Cancer Treatment. Adv. NanoBiomed Res 2021, 2000089, 2000089. 10.1002/anbr.202000089.

(21). Barenholz Y Liposome Application: Problems and Prospects. Curr. Opin. Colloid Interface Sci 2001, 6 (1), 66–77. 10.1016/S1359-0294(00)00090-X.

(22). Ahmed SE; Martins AM; Husseini GA The Use of Ultrasound to Release Chemotherapeutic Drugs from Micelles and Liposomes. J. Drug Target 2015, 23 (1), 16–42. 10.3109/1061186X.2014.954119. [PubMed: 25203857]

(23). Zylberberg C; Matosevic S Pharmaceutical Liposomal Drug Delivery: A Review of New Delivery Systems and a Look at the Regulatory Landscape. Drug Deliv. 2016, 23 (9), 3319–3329. 10.1080/10717544.2016.1177136. [PubMed: 27145899]

(24). Awad NS; Paul V; Mahmoud MS; Al Sawaftah NM; Kawak PS; Al Sayah MH; Husseini GA Effect of Pegylation and Targeting Moieties on the Ultrasound-Mediated Drug Release

from Liposomes. ACS Biomater. Sci. Eng 2020, 6 (1), 48–57. 10.1021/acsbiomaterials.8b01301. [PubMed: 33463192]

(25). Kono K; Takashima M; Yuba E; Harada A; Hiramatsu Y; Kitagawa H; Otani T; Maruyama K; Aoshima S Multifunctional Liposomes Having Target Specificity, Temperature-Triggered Release, and near-Infrared Fluorescence Imaging for Tumor-Specific Chemotherapy. J. Control. Release 2015, 216, 69–77. 10.1016/j.jconrel.2015.08.005. [PubMed: 26264832]

(26). Mirahmadi N; Babaei MH; Vali AM; Dadashzadeh S Effect of Liposome Size on Peritoneal Retention and Organ Distribution after Intraperitoneal Injection in Mice. Int. J. Pharm 2010, 383 (1–2), 7–13. 10.1016/j.ijpharm.2009.08.034. [PubMed: 19729056]

(27). Litzinger DC; Buiting AMJ; Van Rooijen N; Huang L Effect of Liposome Size on the Circulation Time and Intraorgan Distribution of Amphipathic Poly(Ethylene Glycol)-Containing Liposomes. Biochim. Biophys. Acta 1994, 1190, 99–107. [PubMed: 8110825]

(28). Juliano RL; Stamp D The Effect of Particle Size and Charge on the Clearance Rates of Liposomes and Liposome Encapsulated Drugs. Biochem. Biophys. Res. Commun 1975, 63 (3), 651–658. 10.1016/S0006-291X(75)80433-5. [PubMed: 1131256]

(29). Allen TM; Everest JM Effect of Liposome Size and Drug Release Properties on Pharmacokinetics of Encapsulated Drug in Rats. J. Pharmacol. Exp. Ther 1983, 226 (2), 539–544. [PubMed: 6875864]

(30). Gonzalez Gomez A; Syed S; Marshall K; Hosseinidoust Z Liposomal Nanovesicles for Efficient Encapsulation of Staphylococcal Antibiotics. ACS Omega 2019, 4 (6), 10866–10876. 10.1021/acsomega.9b00825. [PubMed: 31460184]

(31). Szoka FC; Milholland D; Barza M Effect of Lipid Composition and Liposome Size on Toxicity and in Vitro Fungicidal Activity of Liposome-Intercalated Amphotericin B. Antimicrob. Agents Chemother 1987, 31 (3), 421–429. 10.1128/AAC.31.3.421. [PubMed: 3579259]

(32). Pei Y; Wei MY; Cheng B; Liu Y; Xie Z; Nguyen K; Yuan B High Resolution Imaging beyond the Acoustic Diffraction Limit in Deep Tissue via Ultrasound-Switchable NIR Fluorescence. Sci. Rep 2014, 4, 4690. 10.1038/srep04690. [PubMed: 24732947]

(33). Saxena V; Sadoqi M; Shao J Enhanced Photo-Stability, Thermal-Stability and Aqueous-Stability of Indocyanine Green in Polymeric Nanoparticulate Systems. J. Photochem. Photobiol. B Biol 2004, 74 (1), 29–38. 10.1016/j.jphotobiol.2004.01.002.

(34). Lu Y; Aimetti AA; Langer R; Gu Z Bioresponsive Materials. Nat. Rev. Mater 2016, 2 (1). 10.1038/natrevmats.2016.75.

(35). Sułkowski WW; Pentak D; Nowak K; Sułkowska A The Influence of Temperature, Cholesterol Content and PH on Liposome Stability. J. Mol. Struct 2005, 744–747 (SPEC. ISS.), 737–747. 10.1016/j.molstruc.2004.11.075.

(36). Fang X; Liu W; Wu X; Zhou W; Chen J; Liu X; Xu Z One-Step Condensation Synthesis and Characterizations of Indocyanine Green. Results Chem. 2021, 3 (November 2020), 100092. 10.1016/j.rechem.2020.100092.

(37). Nkanga CI; Bapolisi AM; Okafor NI; Krause RWM General Perception of Liposomes: Formation, Manufacturing and Applications. In Liposomes: Advances and Perspectives; IntechOpen, 2019.

(38). Maruyama K Intracellular Targeting Delivery of Liposomal Drugs to Solid Tumors Based on EPR Effects. Adv. Drug Deliv. Rev 2011, 63 (3), 161–169. 10.1016/j.addr.2010.09.003. [PubMed: 20869415]

(39). Bachmann MF; Jennings GT Vaccine Delivery: A Matter of Size, Geometry, Kinetics and Molecular Patterns. Nat. Rev. Immunol 2010, 10 (11), 787–796. 10.1038/nri2868. [PubMed: 20948547]

(40). Yoshioka H Surface Modification of Haemoglobin-Containing Liposomes with Polyethylene Glycol Prevents Liposome Aggregation in Blood Plasma. Biomaterials 1991, 12 (9), 861–864. 10.1016/0142-9612(91)90075-L. [PubMed: 1764558]

(41). Gabizon AA Liposome Circulation Time and Tumor Targeting: Implications for Cancer Chemotherapy. Adv. Drug Deliv. Rev 1995, 16 (2–3), 285–294. 10.1016/0169-409X(95)00030-B.

(42). Maitani Y; Aso Y; Yamada A; Yoshioka S Effect of Sugars on Storage Stability of Lyophilized Liposome/DNA Complexes with High Transfection Efficiency. Int. J. Pharm 2008, 356 (1–2), 69–75. 10.1016/j.ijpharm.2007.12.033. [PubMed: 18249511]

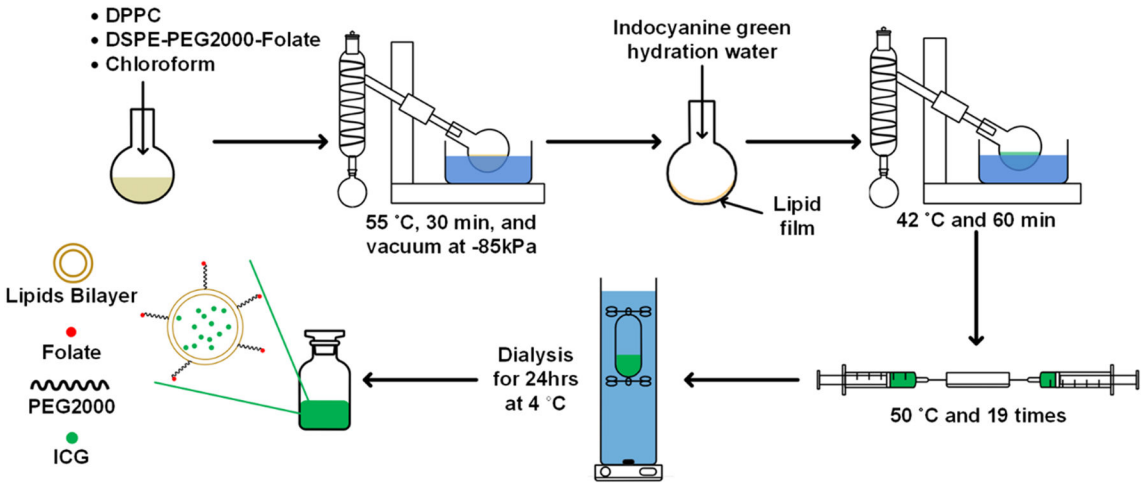

Figure 1.
The schematic diagram of synthesizing PEGylated and ICG-encapsulated liposomes.

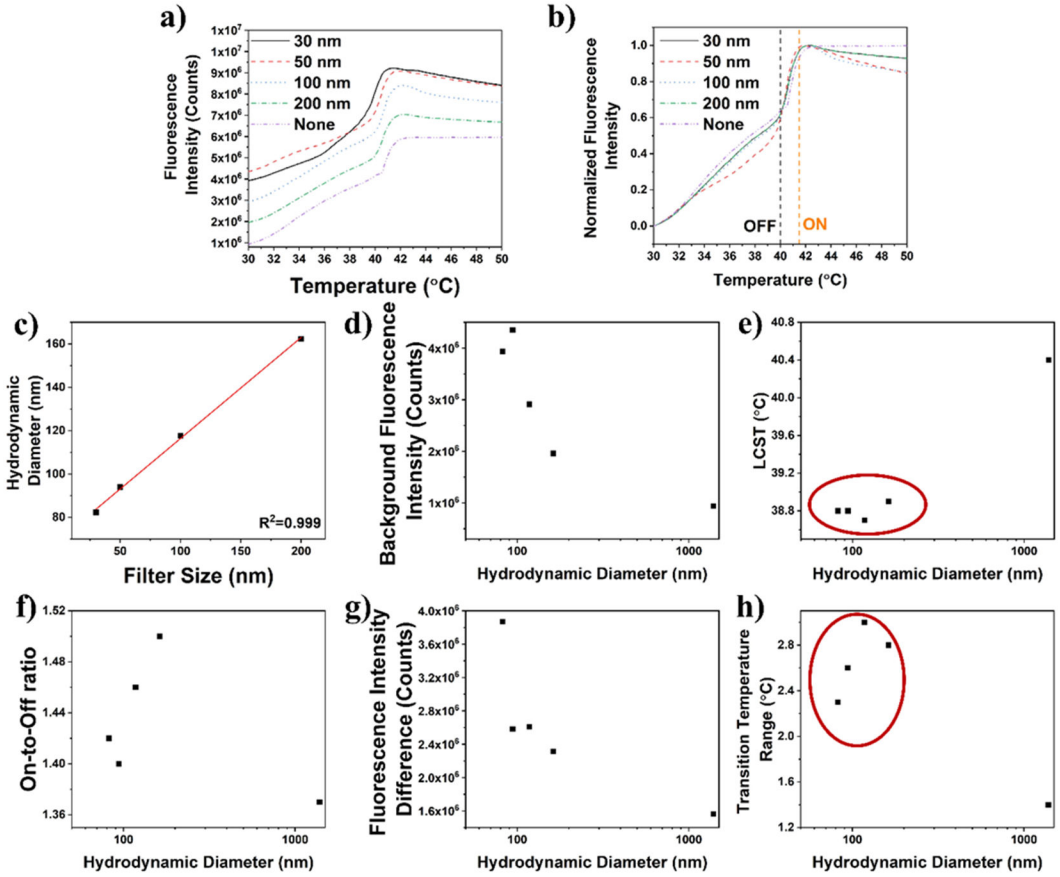

Figure 2.

The fluorescence intensity profile of ICG-liposomes synthesized using different sized filters (30, 50, 100, and 200 nm) and unfiltered ICG-liposomes: a) the profile of the emitted fluorescence intensity change corresponding to the change of temperature; b) normalized fluorescence intensity changes with respect to the change in temperature; c) the relationship between the hydrodynamic size of ICG-liposomes and filter size used during extrusion; d) the background fluorescence intensity of different sized ICG-liposomes; e) the size effect on LCST of ICG-liposomes; f) the correlation between the on-to-off ratio and the size of ICG-liposomes; g) the size effect on the absolute fluorescence intensity difference between switched on and off; and h) the size effect on the transition temperature range. “None” represents not filtered ICG-liposomes.

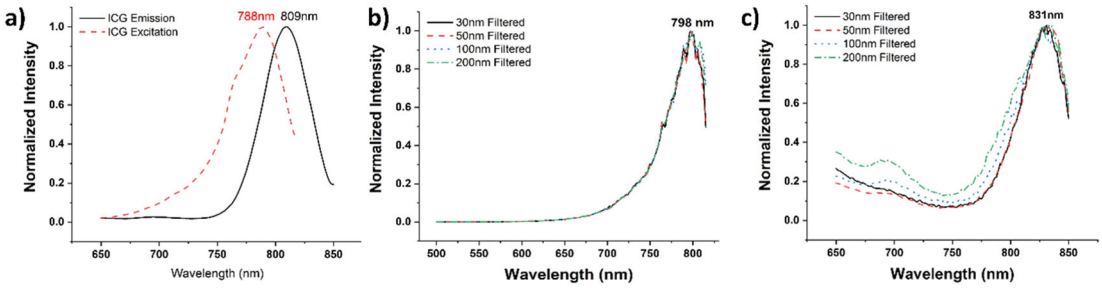

Figure 3.

a) Excitation and emission spectra of fresh ICG aqueous solution, b) excitation spectrum, and c) emission spectrum for various sized ICG-liposomes.

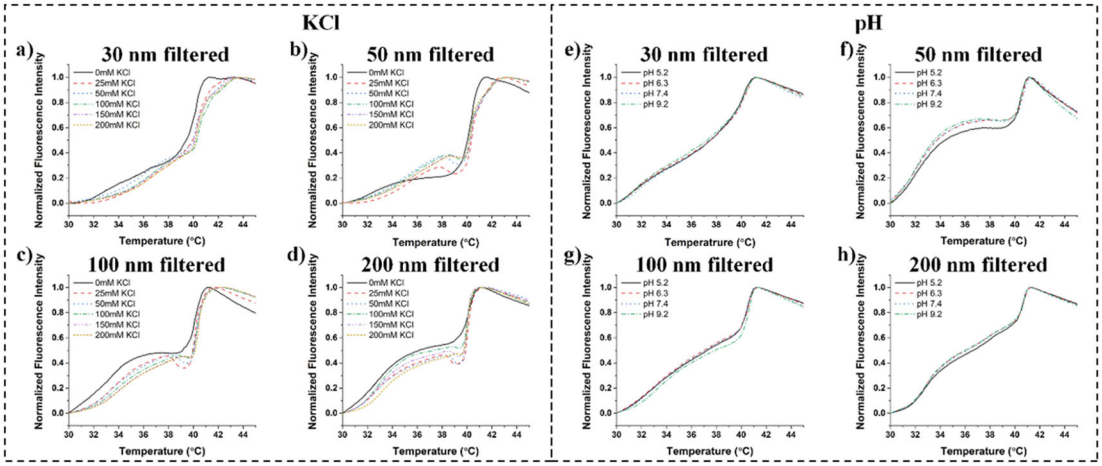

Figure 4.

The effect of ionic strengths (KCl) on the stability of a) 30 nm, b) 50 nm, c) 100 nm, and d) 200 nm filtered ICG-liposomes. The effects of different pH values on the stability of e) 30 nm, f) 50 nm, g) 100nm, and h) 200 nm filtered ICG-liposomes.

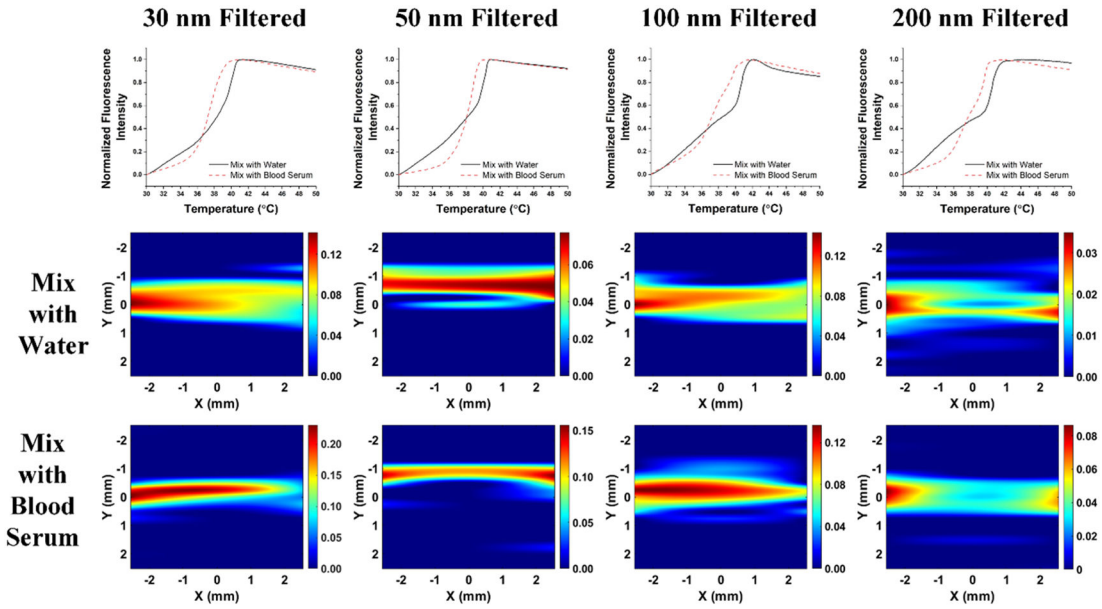

Figure 5.

Fluorescence intensity profile measured with the in-house built cuvette system and USF imaging of different sized ICG-liposomes mixed with either water or blood serum.

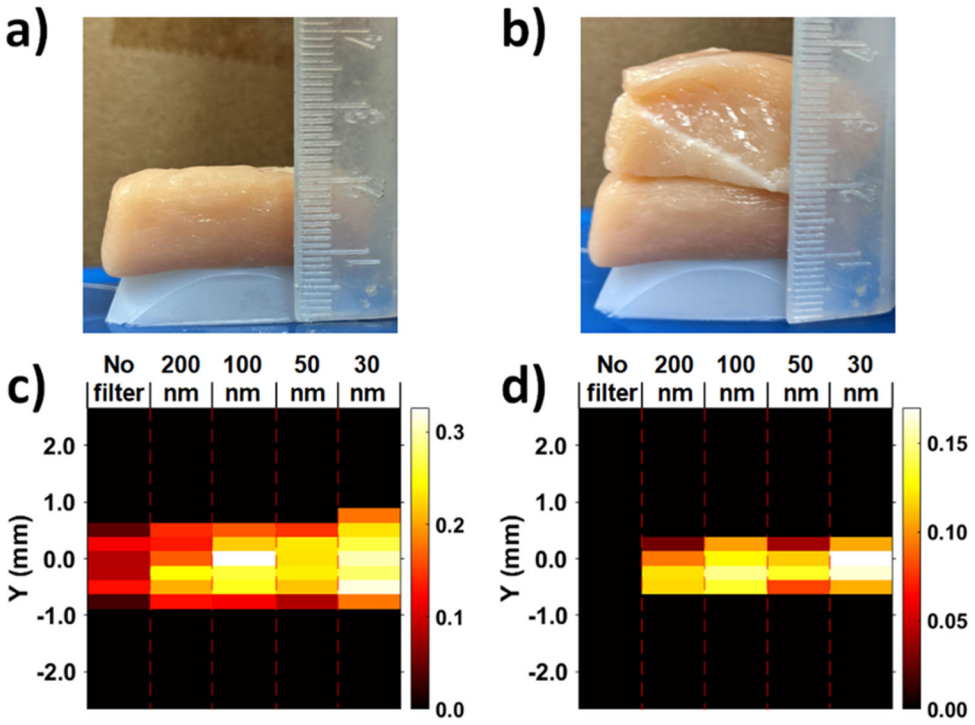

Figure 6.

USF imaging of various-sized ICG-liposomes at different depths. The silicone tube-embedded silicone phantoms with a thickness of a 0.8 cm were stacked with a) 1.0 cm or b) 2.5 cm thick chicken breast tissue. The USF imaging of unfiltered ICG-liposomes and ICG-liposomes, which were filtered with 30, 50, 100, and 200 nm filter discs at c) 1.0 cm and d) 2.5 cm.

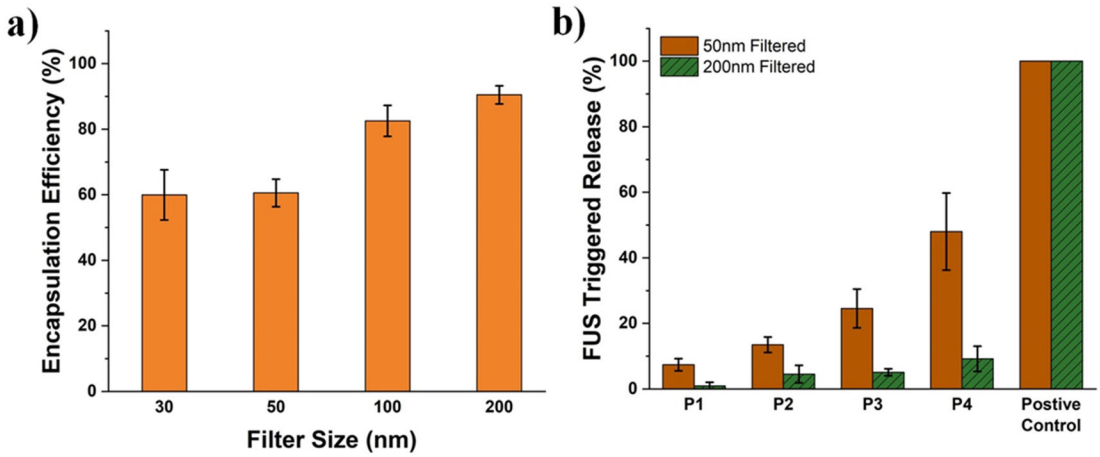

	Ultrasound Power (W)	Mechanical Index	Exposure Time (min)
P1	0.19	0.97	25
P2	1.74	2.90	25
P3	4.82	4.83	25
P4	4.82	4.83	125

Figure 7.

a) Encapsulation efficiency of various-sized ICG-liposomes; b) ultrasound-triggered ICG release for 50 nm and 200 nm filtered ICG-liposomes. FUS power conditions used during the releasing test included P1: 0.19 W (MI 0.97), P2: 1.74 W (2.90), P3: 4.82 W (MI 4.83), and P4: 4.82 W (MI 4.83; repeated five times). The number of replicates was n = 3.